PROCEEDINGS OF THE ROYAL SOCIETY A MATHEMATICAL, PHYSICAL & ENGINEERING SCIENCES

Vacuum Ultra-Violet Flash Photolysis of Water Vapour

G. Black and G. Porter

Proc. R. Soc. Lond. A 1962 **266**, 185-197
doi: 10.1098/rspa.1962.0055

Vacuum ultra-violet flash photolysis of water vapour

By G. Black and G. Porter, F.R.S.

Department of Chemistry, University of Sheffield

(*Received* 6 *September* 1961)

An apparatus for effecting flash photolysis in the vacuum ultra-violet region is described. Appreciable decompositions of water, carbon dioxide, acetylene, ethylene and methane were effected with a 2000 J flash of 30 μs duration.

A detailed study of water vapour photolysis has established that, in the primary step, at least 90 % of the dissociation leads to a hydrogen atom and a hydroxyl radical. The kinetics of the hydroxyl radical disappearance, following flash photolysis of water vapour in the presence of various third bodies, has been studied. The rate constant is faster in xenon than in helium and other similarities with the data on iodine atom recombination suggest the operation of a mechanism involving intermediate complex formation.

Introduction

The technique of flash photolysis, as at present applied, generally suffers from the limitation of being applicable only to molecules absorbing at wavelengths greater than 2000 Å. Light of shorter wavelengths is absorbed by the quartz walls of the photolysis flash lamp and reaction cell and by the air between the lamp and cell. The first aim of the present work was to devise an apparatus capable of effecting flash photolysis in the vacuum ultra-violet region.

Some previous work has been carried out with the object of extending flash photolysis to this region. Nelson & Ramsay (1956) used a sapphire flash tube mounted inside a Pyrex reaction vessel but, although sapphire has good optical properties and transmits down to about 1435 Å (Freed, McMurry & Rosenbaum 1939), they found that its mechanical properties were inferior to those of quartz and that its transparency rapidly deteriorated on flashing. Energies much in excess of 100 J were found to roughen the internal surface of the sapphire lamp, whereas 1000 to 5000 J discharges cause little change in quartz lamps. They concluded that, with the exception of CN obtained from photolysis of HCN, the radicals which they observed were produced by an electrical discharge along the outside of the lamp and not by photolysis. Schüler & Krimmel (1957) used a discharge in the reaction vessel itself. They used a magnetic field to confine the discharge and observed radical absorption some distance away. The presence of a shock wave after the discharge complicates this system and the effects observed cannot be attributed unambiguously to photochemical dissociation. A system for effecting vacuum ultra-violet flash photolysis has recently been described by Bortner, Povard & Myerson (1960). Using a thin-walled fused quartz flash tube running co-axially through the reaction cell, they were able to effect the photodecomposition of carbon dioxide. The system was not, however, designed to study the transients present after flash photolysis.

The approach adopted in this work was to use a reaction cell which was transparent to the vacuum ultra-violet region and to dispense with the tube constraining the flash discharge. Originally, it was thought that the best material from which to

construct the reaction cell would be sapphire. This would utilize the good optical properties of sapphire and would not require the exacting mechanical properties which are required if the flash lamp itself is constructed from this material. However, recent developments in the removal of alumina from silica have resulted in a quartz with high transmission to less than 1500 Å and this material was chosen for the reaction cell. The cell was surrounded by a cylindrical vessel filled with argon through which the discharge passed. Flash spectroscopic recording, in the range 2250 to 6600 Å, was effected in the conventional manner.

Experimental

A schematic diagram of the apparatus is shown in figure 1. The cylindrical Pyrex vessel, *B* (approximately 18 cm outside diameter, 15 cm length and 1 cm thick walls) had metal plates, *D*, machined to fit over its ends. Synthetic hard-rubber

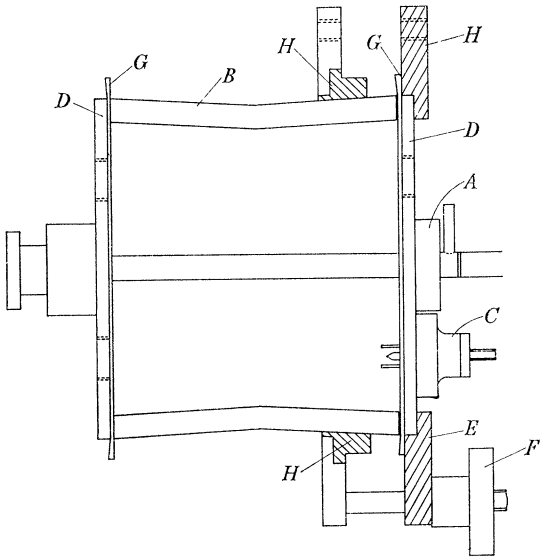

Figure 1. Schematic diagram of vacuum ultra-violet flash photolysis apparatus. *A*, cell holder assembly; *B*, Pyrex vessel; *C*, electrode assembly; *D*, end-plates; *E*, clamps to end-plates; *F*, quick release nuts; *G*, gasket; *H*, rubber ring.

gaskets, *G*, were fitted between the end-plates and the Pyrex. The vessel was held together by three clamping arrangements, *E*, operated by quick-release nuts, *F*, on each end-plate. The reaction cell passed co-axially through the vessel. O-ring seals were used in the holding assemblies at each end of the cell.

Four electrodes, of the type shown in figure 2, were screwed into each end-plate. The electrode body was made of brass into which a pointed tungsten rod was soldered. It was insulated from the end-plate by the main body of the electrode made from Silvonite, a silica-loaded ebonite. Each electrode incorporated two O-ring seals, as shown, to give a vacuum-tight assembly when screwed into the end-plate. In order to prevent the sputtering of metal from the tip of the tungsten rod on to the reaction cell, the rod was shielded by a quartz sleeve. The sleeve was

first fixed in position by running paraffin wax down between it and the main body. The paraffin wax was then covered with a layer of Araldite. It was found that the discharge would occasionally jump to the end-plates. This resulted in sputtered metal, some of which finally settled on the cell, giving an absorbing layer. The trouble was overcome by covering the end-plates with a layer of a glass fibre adhesive ('Tetra-bond').

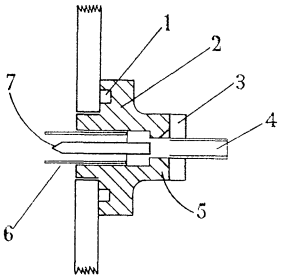

FIGURE 2. Electrode assembly. 1, O-ring; 2, main body; 3, compression plate; 4, electrode body; 5, O-ring; 6, quartz sleeve; 7, tungsten rod.

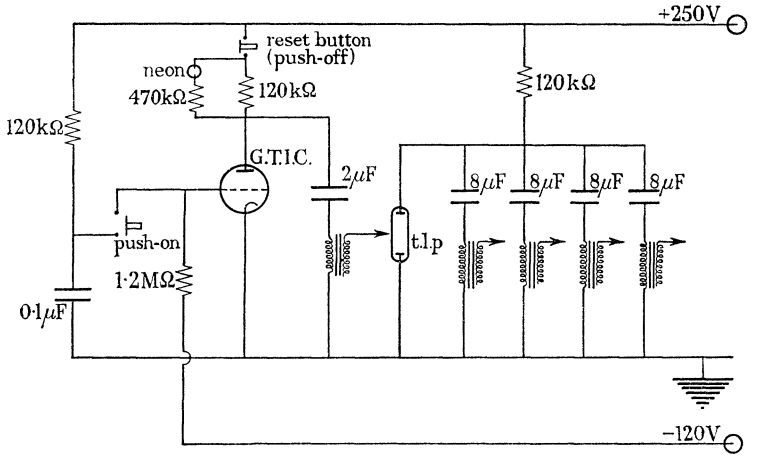

FIGURE 3. Trigger unit. (t.l.p. = telephone-line protector.)

The vessel was pumped down to a pressure of less than 10^{-3} mm and then filled with argon at a pressure of about 60 mm. Each of the four pairs of electrodes had its own spark gap and a 10 μF condenser, which could be charged to 10 kV, provided the power source. To trigger all the spark gaps simultaneously, the four separate trigger circuits, each incorporating an 8 μF condenser charged to 250 V and a Dawe pulse transformer, all had a common hold-off spark gap. This was a gas-filled telephone-line protector. The circuit diagram is shown in figure 3. Ionization of this gap therefore initiated a photo-flash of 2000 J energy. The resulting light pulse had a 30 μs half-peak height duration.

The spectroscopic flash lamp had a central capillary section. The light from this section was collimated with a 3 cm focal length quartz lens. One flash of 4 μF at 8 kV was sufficient to give reasonable intensity from 2300 to 4750 Å on Ilford HP 3

plates with a 2 m normal incidence grating spectrograph and a 20 μ slit width. From 4750 to 6600 Å, five flashes were required. Appropriate filters were used to prevent an overlap of orders. The half-peak height duration of this flash was 20 μs.

Results

Actinometry

Some preliminary work was carried out to ascertain the dependence of the light output on the discharge length and on the argon pressure. Figure 4 shows the variation with the discharge length measured by the use of carbon dioxide as

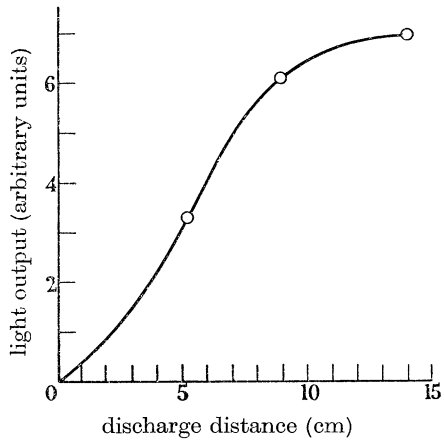

Figure 4. Graph of light output, measured by carbon dioxide decomposition, against discharge distance.

actinometer. In our final arrangement, the gap length was made as large as possible (14 cm). The light output was also found to increase slightly with increasing argon pressure. In the work to be described, pressures between 6 and 12 cm of argon were used, the upper limit being set by the danger of exploding the vessel.

A graph of decomposition against carbon dioxide pressure is shown in figure 5. The amount of decomposition was determined by freezing out the carbon dioxide in a liquid-nitrogen trap and measuring the residual gas. A check that the amounts of oxygen and carbon monoxide were in the ratio 1 : 2 was carried out by combustion in a copper/copper oxide furnace at 240 °C when the carbon monoxide is oxidized to carbon dioxide and the oxygen is removed.

The graph indicates that a maximum decomposition of about 0·10 mm of carbon dioxide in a cell of volume 32·2 ml. can be obtained. Using Mahan's (1960) value of unity for the quantum yield of carbon dioxide photolysis, allowing for the solid angle subtended by the cell at the discharge path and neglecting any reflexion from the Pyrex walls, we obtain a total emission of $2{\cdot}2 \times 10^{18}$ quanta in the region of absorption of carbon dioxide below 1690 Å. This is equivalent to at least 2·9 J of the 500 J discharge, or, 0·6 %, which compares favourably with the 0·4 % reported by Bortner *et al.* (1960).

Some less exact actinometric work with ammonia, with the use of Wiig & Kistiakowsky's (1932) value of 0·25 for the quantum yield, indicated that about 5 % of the stored energy appeared as radiation of wavelength less than 2200 Å. This is an upper limit because the quantum yield below 1900 Å is higher than 0·25 (Kassel & Noyes 1927).

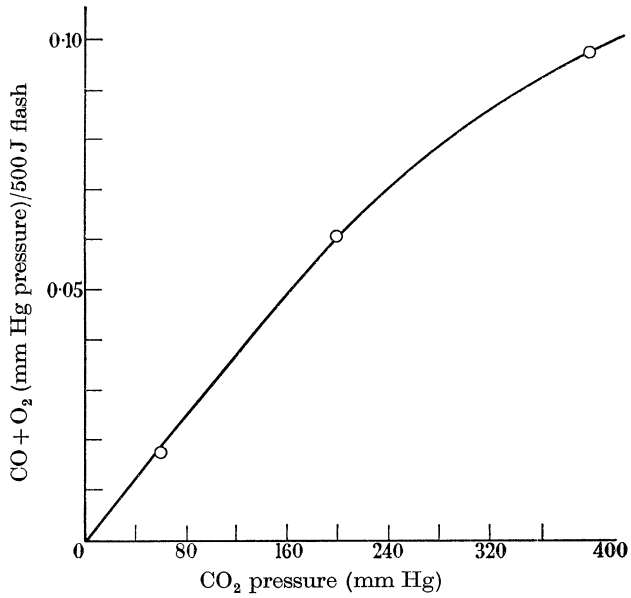

FIGURE 5. Graph of decomposition against carbon dioxide pressure.

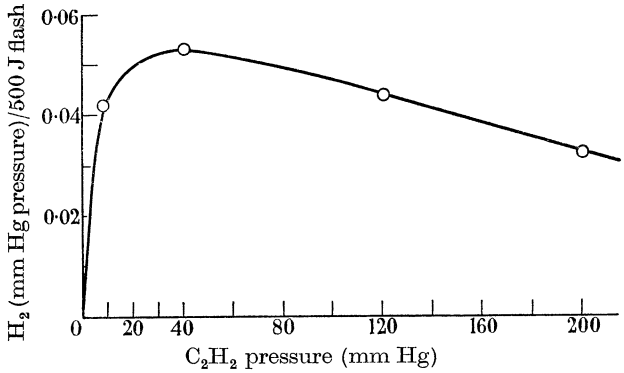

FIGURE 6. Graph of decomposition against acetylene pressure.

Acetylene, ethylene, water vapour and methane

Graphs of decomposition against pressure of acetylene, ethylene and water vapour are shown in figures 6, 7 and 8, respectively. The absorption spectra of these molecules are such that only light of wavelengths less than 1900 Å will be effecting appreciable decomposition.

The sections of negative slope on the acetylene and ethylene graphs indicate a falling quantum yield of hydrogen production and may be interpreted in terms of

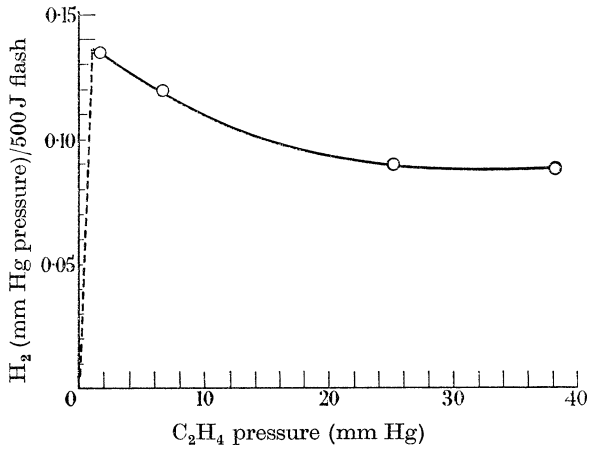

FIGURE 7. Graph of decomposition against ethylene pressure.

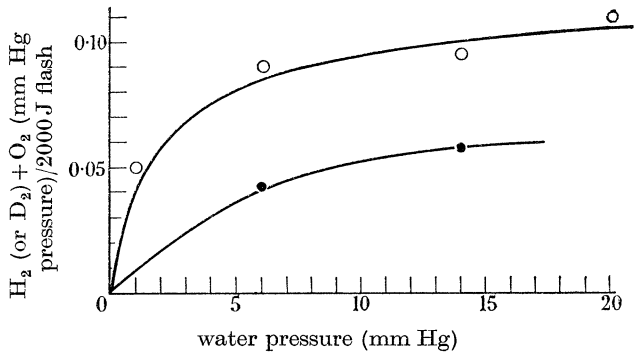

FIGURE 8. Graph of decomposition against water vapour pressure. ○, H_2O; ●, D_2O.

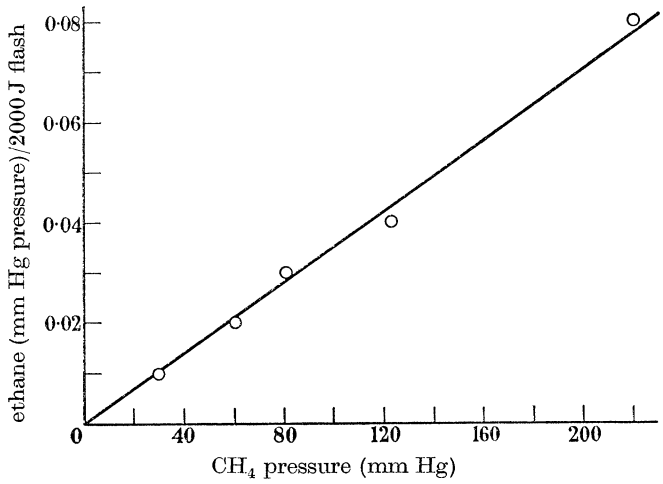

FIGURE 9. Graph of decomposition against methane pressure.

a self-quenching mechanism for the dissociating state. Similar results have been obtained by Zelikoff & Aschenbrand (1956) in the normal photodecomposition of acetylene and by Callear & Cvetanović (1956) in the mercury-photosensitized decomposition of ethylene.

No new transient absorption spectra were observed in these systems. The OH and OD radicals were observed after photolysis of water and heavy water respectively and their detailed study is reported later. From acetylene, a continuous absorption was observed below 2800 Å which increased with the number of flashes and was therefore caused by product formation.

A graph of the ethane produced against methane pressure is shown in figure 9. The ethane was measured after condensing it out in liquid-nitrogen traps and pumping away the methane and hydrogen. The photodecomposition of methane shows that the quartz of the reaction cell is transmitting wavelengths shorter than 1500 Å.

Other systems

As expected, the amino radical was observed 60 μs after flash photolysis of ammonia. On flashing methylamine, a much weaker absorption of the amino radical was seen after 60 μs decay in spite of the fact that methylamine yielded about four times the pressure of non-condensable products obtained from ammonia. The most likely explanation is that methylamine can decompose photochemically by more than one primary act. In fact, Wetmore & Taylor (1944) have suggested

$$CH_3NH_2 + h\nu \rightarrow CH_3NH + H$$

as a primary act.

Although the process

$$CH_3NH_2 \rightarrow CH_3 + NH_2$$

has been postulated as a primary step in the thermal and in the photochemical decomposition of methylamine by Emeleus & Jolley (1935) and by Emeleus & Taylor (1931), respectively, no directly supporting experimental facts have previously been obtained. The observation of the amino radical spectrum can be regarded as good evidence for the occurrence of such a primary step.

Methyl alcohol vapour was also studied. No hydroxyl absorption was observed but a polymeric material, giving off formaldehyde on heating, was formed on the cell walls. Thus the primary process

$$CH_3OH + h\nu \rightarrow CH_3 + OH$$

can be of little importance. This agrees with the recent work of Porter & Noyes (1959) on the photochemistry of methyl alcohol vapour.

Water photolysis and the recombination of OH radicals

Water vapour begins to absorb below 1880 Å and the spectrum consists of a number of diffuse bands superimposed on a continuum. The continuum has an intensity maximum at about 1650 Å and extends down to about 1400 Å (Wilkinson & Johnson 1950).

Early work on water photolysis was interpreted in terms of the dissociation

$$H_2O + h\nu \rightarrow H_2 + O(^1D). \qquad (a)$$

Herzberg (1931), however, pointed out that this was not possible energetically for wavelengths above 1800 Å and that the process

$$H_2O + h\nu \rightarrow H + OH \qquad (b)$$

was most probable for this absorption band. Groth (1939), reviewing the situation, favoured this suggestion. Some recent work by Chen & Taylor (1957) was explained in terms of (*b*). They were able to obtain quantum yields of decomposition as high as 0·3 using a fast flow system.

In the liquid phase, Barrett & Baxendale (1960), using 1849 Å irradiation of aqueous solutions of methanol and ethyl acetate and measuring the quantum yield of hydrogen production, interpreted their results in terms of (*b*) and found it to have a quantum yield of 0·6.

Our observation of OH absorption does not prove the occurrence of process (*b*) since (*a*) might be followed by

$$O + H_2O \rightarrow 2OH \qquad (c)$$

or, after several flashes,

$$O + H_2 \rightarrow OH + H. \qquad (d)$$

Since reaction (*d*) is much faster than (*c*), we can, however, distinguish between (*a*) and (*b*) by photolysis of a heavy water/hydrogen mixture. In such a system reaction (*a*) followed by (*d*) will give OH whereas (*b*) will give OD. With a mixture of 10 mm pressure of heavy water and 5 mm pressure of hydrogen, only OD radical absorption was observed at 60 μs delay. The limit of detection of OH was approximately one-tenth of the observed OD concentration which establishes that at least 90 % of the primary dissociation occurs via process (2).

Kinetics of hydroxyl disappearance

After the flash photolysis of water, the following homogeneous gas phase reactions are possible

$$H + H + M \xrightarrow{k_1} H_2 + M, \qquad (1)$$

$$H + OH + M \xrightarrow{k_2} H_2O + M, \qquad (2)$$

$$OH + OH + M \xrightarrow{k_3} H_2O_2 + M. \qquad (3)$$

From these equations, we have

$$-\frac{d[OH]}{dt} = k_2[OH][H][M] + 2k_3[OH]^2[M].$$

At the beginning of the reaction, [H] = [OH], and

$$-\frac{d[OH]}{dt} = k[OH]^2[M], \quad \text{where} \quad k = k_2 + 2k_3.$$

Calibration of the intensity of hydroxyl radical absorption

Using cells of path length l, $\frac{1}{2}l$, $\frac{1}{4}l$ and $\frac{1}{8}l$ cm, the same pressure of water vapour (14 mm), the same photolysis conditions and recording the absorption spectrum at a constant time after the peak of the photolysis flash (40 μs delay), spectra corresponding to concentrations $[OH]_0$, $\frac{1}{2}[OH]_0$, $\frac{1}{4}[OH]_0$ and $\frac{1}{8}[OH]_0$ in the original path length l cm were obtained. These spectra were then matched visually with those recorded during a kinetic experiment.

A kinetic experiment involved filling the cell with 14 mm pressure of water vapour and a known pressure of inert gas or other third body. Flash spectroscopic records of the hydroxyl absorption at varying delays were obtained using a fresh mixture for each delay. The photographic plates were then processed by a standardized procedure.

Results

(*a*) *Inert gases*

Plots of $1/[OH]_t$ against time were linear and third-order kinetics were found to be obeyed throughout the range of inert gas pressures studied (10 to 80 cm pressure).

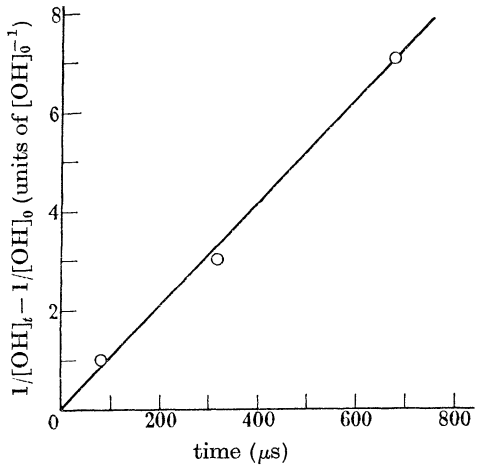

Figure 10. Rate of disappearance of hydroxyl in a mixture of 14 mm pressure of water vapour and 186 mm pressure of argon.

This agrees with the work of Frost & Oldenberg (1936). A typical plot for an argon/water mixture is shown in figure 10. The fact that the plots are linear over an eightfold range of [OH] indicates either that $k_2 \ll k_3$ or that the overall rates of removal of H and OH are similar.

For the inert gas/water mixture, we have

$$k[M] = k_g[\text{inert gas}] + k_{H_2O}[H_2O],$$

$$k = k_g + k_{H_2O}\frac{[H_2O]}{[\text{inert gas}]}.$$

Plots of $[H_2O]/[\text{inert gas}]$ against k for helium, argon and xenon are shown in figure 11. This plot gives k_g as the intercept and k_{H_2O} as the reciprocal of the slope.

Deviations from the straight lines at the higher $[H_2O]/[\text{inert gas}]$ ratios, that is at the lower inert-gas pressures, can be interpreted in terms of a thermal effect—the energy liberated by the recombining radicals heating up the gas and causing migration of the radicals towards the cold walls.

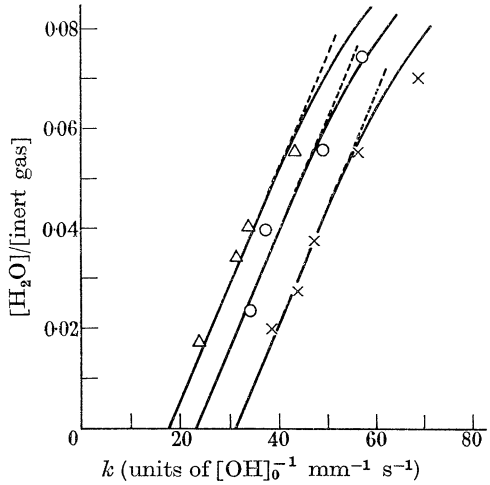

FIGURE 11. Graph to determine the third-order rate constant, k, for helium, argon, xenon and water as third bodies. △, Helium; ○, argon; ×, xenon.

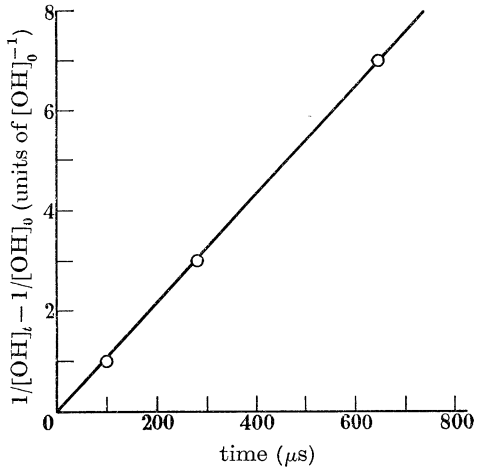

FIGURE 12. Rate of disappearance of hydroxyl in a mixture of 14 mm pressure of water vapour and 71 mm pressure of nitrogen.

(*b*) *Other chaperon molecules*

Good third-order plots were obtained for nitrogen (figure 12). Only low pressures of oxygen and carbon dioxide could be used because they absorb in the same region as water vapour and the light absorbed gives oxygen atoms which complicate the reaction sequence. For these two third-bodies, the large thermal effect, and, possibly, reactions of the oxygen atoms, gave rise to curved plots and the rate

constant was determined from the slope of the tangent to the graph at the origin—this removes the thermal effect but does not circumvent the possible effects of oxygen atom reactions.

The results obtained are shown in the second column of table 1. An upper limit for the absolute value for water can be set from the decomposition against water-vapour pressure graph (figure 8). Since the measured decomposition product is mainly hydrogen (Chen & Taylor 1957), this sets a minimum hydrogen atom pressure of 0·1 mm and therefore a minimum hydroxyl radical pressure of 0·1 mm and thus an upper limit for k_{H_2O} of 4200 $mm^{-2}\,s^{-1}$.

Taking Oldenberg & Rieke's (1939) absolute value for water as the third body of 1400 $mm^{-2}\,s^{-1}$, we obtain the absolute value for the other third bodies, as shown in the third column of table 1.

TABLE 1

third body	$k[OH]_0$ ($mm^{-1}\,s^{-1}$) ($k = k_2 + 2k_3$)	k ($mm^{-2}\,s^{-1}$)	$\frac{k_2}{k_3}$	k_3 ($mm^{-2}\,s^{-1}$)	$10^{32}\,k_3$ (ml.^{2} $mol.^{-2}\,s^{-1}$)	$10^{32}\,k$ for $I + I + M$
helium	17·5	58	2·55	13	1·3 ± 0·15	0·4
argon	23	77	2·96	16	1·5 ± 0·2	0·8
xenon	31	103	3·18	20	2·0 ± 0·2	1·5
nitrogen	77	257	2·89	53	5·1 ± 0·5	1·3
oxygen	120 ± 30	400 ± 100	2·9	82 ± 20	7·9 ± 2·0	1·9
carbon dioxide	100 ± 35	330 ± 110	3·0	66 ± 20	6·4 ± 2·0	3·8
water	420	1400	2·79	292	28·2 ± 2·8	13·7

DISCUSSION

The results in columns (2) and (3) of table 1 show an interesting parallelism with the efficiency of third bodies in iodine atom recombination given in the last column of the table (Russell & Simons 1953; Porter & Smith 1961). The same order for the inert gases is obtained and the same high efficiency of water is found. This contrasts with the data on methyl radical recombination where the rate in helium is at least a factor of two greater than the rate in argon (Ingold, Henderson & Lossing 1953; Dodd & Steacie 1954).

Iodine atom and methyl radical recombinations are representative of the two types of mechanism encountered in non-radiative, that is, third-order, recombinations of atoms and radicals. It has been shown (Porter & Smith 1961) that iodine atom recombination probably involves the participation of a charge transfer complex of the third body and an iodine atom in the recombination step. The full mechanism can be written

$$I + M \rightleftharpoons IM,$$

$$IM + I \rightarrow I_2 + M.$$

Methyl radical recombination involves the collisional stabilization of an excited ethane molecule formed by the association of two methyl radicals. The full mechanism can be written

$$CH_3 + CH_3 \rightleftharpoons C_2H_6^*,$$

$$C_2H_6^* + M \rightarrow C_2H_6 + M.$$

The correspondence with the iodine atom rates and the lack of similarity with the methyl radical rates suggests that the mechanism of hydroxyl radical disappearance resembles that of iodine atom recombination. This probably requires the participation of a charge transfer complex in the recombination step. Of the two reactive species present in the water vapour system, the hydrogen atom and the hydroxyl radical, the latter has a much higher electron affinity, 61 kcal/mole (Page & Sugden 1957) than the former 17 to 23 kcal/mole (Mann, Hustrulid & Tate 1940; Pritchard 1953), and is thus favoured as the complexing species. In fact, the electron affinity of the hydroxyl radical approaches that of the iodine atom, 77 kcal/mole (Bakulina & Ionov 1955).

Assuming the hydroxyl complex as one of the species in the recombination steps, the detailed mechanisms of (2) and (3) both involve the first two steps,

$$\mathrm{OH} + M \rightarrow \mathrm{OH}.M, \tag{4}$$

$$\mathrm{OH}.M \rightarrow \mathrm{OH} + M, \tag{5}$$

and only differ in the third step,

$$\mathrm{OH}.M + \mathrm{H} \rightarrow \mathrm{H_2O} + M, \tag{6}$$

$$\mathrm{OH}.M + \mathrm{OH} \rightarrow \mathrm{H_2O_2} + M. \tag{7}$$

The ratio of k_2 to k_3 will then be the ratio of k_6 to k_7. These reactions are likely to be very efficient and their relative rate is probably close to their relative collision rate. Kinetic theory calculations of this ratio using $\sigma_{\mathrm{H}} = 2{\cdot}5\,\text{Å}$ and $\sigma_{\mathrm{OH}} = 3{\cdot}1\,\text{Å}$ are given in column (4) of table 1. From this ratio, k_2 and k_3 may be separately determined and values of k_3 are shown in columns five and six.

Radical and atom recombination reactions, proceeding by either the mechanism of iodine atom or methyl radical recombination, have small negative activation energies. An attempt was made to show this for the recombination reactions proceeding after the flash photolysis of water vapour. Heating the reaction cell contents was attempted by circulating these through the heated entrance tube of the reaction cell with a Töpler pump. Although the entrance tube was heated to 200 to 250 °C, the heat losses were such that the cell contents could only be heated to 20 to 25 °C, and this was considered insufficient to study the negative activation energy effect.

Previous work on these reactions is somewhat limited. Oldenberg & Rieke (1939), in addition to determining $k_{\mathrm{H_2O}} = 1400\,\mathrm{mm^{-2}\,s^{-1}}$ also obtained $k_{\mathrm{He}} = 600\,\mathrm{mm^{-2}\,s^{-1}}$. This is about ten times the value obtained here. The difference may arise from complications resulting from the use of electrical discharge excitation. Ziskin & Kondratiev (1936) have determined $k_{\mathrm{H_2O}} = 9900\,\mathrm{mm^{-2}\,s^{-1}}$. This is greater than the maximum value of $4200\,\mathrm{mm^{-2}\,s^{-1}}$ predicted from the decomposition against water-vapour pressure graph.

Bulewicz & Sugden (1958), studying hydrogen flames, obtained data on k_2 with water as the third body. They were also able to show that water was a much more efficient third body than nitrogen and hydrogen. Their data were obtained in the temperature range 1650 to 2300 °K and showed the negative temperature coefficient characteristic of atom and radical recombination reactions. Their results for

$k_{2(H_2O)}$ ranged from $1{\cdot}5 \times 10^{-31}$ ml.^{2} molecule^{-2} s^{-1} at 2300 °K to $1{\cdot}5 \times 10^{-30}$ ml.^{2} molecule^{-2} s^{-1} at 1650 °K. Oldenberg & Rieke's (1939) value of k_{H_2O} at 300 °K, together with the ratio $k_2/k_3 = 2{\cdot}79$ from table 1, gives $k_2 = 0{\cdot}79 \times 10^{-30}$ ml.^{2} molecule^{-2} s^{-1}. In view of the widely different temperatures and conditions and as the rate of radical recombination changes only slowly with temperature, the agreement between these two results can be considered to be fairly satisfactory.

It therefore appears that a mechanism similar to that involved in iodine atom recombination, and probably involving a charge transfer complex of the hydroxyl radical and third body, plays an important part in the recombination of hydroxyl radicals and, also, in the recombination of a hydrogen atom and a hydroxyl radical. Since the range of rates in the inert gases is not so marked as in the iodine atom recombination and since there is a different order of rates in xenon and nitrogen, some recombination probably proceeds via collisional stabilization of $H_2O_2^*$ and H_2O^*.

One of the authors (G. B.) is grateful to the University of Sheffield for the award of the Charles Kingston Everitt Memorial Scholarship during the period of this research.

References

Bakulina, I. N. & Ionov, N. I. 1955 *Dokl. Akad. Nauk. S.S.S.R.* **105**, 680.
Barrett, J. & Baxendale, J. H. 1960 *Trans. Faraday Soc.* **56**, 37.
Bortner, M. H., Povard, V. D. & Myerson, A. L. 1960 *J. Opt. Soc. Amer.* **50**, 172.
Bulewicz, E. M. & Sugden, T. M. 1958 *Trans. Faraday Soc.* **54**, 1855.
Callear, A. B. & Cvetanović, R. J. 1956 *J. Chem. Phys.* **24**, 873.
Chen, M. C. & Taylor, H. A. 1957 *J. Chem. Phys.* **27**, 857.
Dodd, R. E. & Steacie, E. W. R. 1954 *Proc. Roy. Soc.* A, **223**, 283.
Emeleus, H. J. & Jolley, L. J. 1935 *J. Chem. Soc.* p. 929.
Emeleus, H. J. & Taylor, H. S. 1931 *J. Amer. Chem. Soc.* **53**, 3370.
Freed, S., McMurry, H. L. & Rosenbaum, E. J. 1939 *J. Chem. Phys.* **7**, 853.
Frost, A. A. & Oldenberg, O. 1936 *J. Chem. Phys.* **4**, 642.
Groth, W. E. 1939 *Z. Elektrochem.* **45**, 262.
Herzberg, G. 1931 *Trans. Faraday Soc.* **27**, 403.
Ingold, K. U., Henderson, I. H. S. & Lossing, F. P. 1953 *J. Chem. Phys.* **21**, 2239.
Kassel, L. S. & Noyes, W. A., Jr. 1927 *J. Amer. Chem. Soc.* **49**, 2495.
Mahan, B. H. 1960 *J. Chem. Phys.* **33**, 959.
Mann, M. M., Hustrulid, A. & Tate, J. T. 1940 *Phys. Rev.* **58**, 340.
Nelson, L. S. & Ramsay, D. A. 1956 *J. Chem. Phys.* **25**, 372.
Oldenberg, P. & Rieke, F. F. 1939 *J. Chem. Phys.* **7**, 485.
Page, F. M. & Sugden, T. M. 1957 *Trans. Faraday Soc.* **53**, 1092.
Porter, G. & Smith, J. A. 1961 *Proc. Roy. Soc.* A, **261**, 28.
Porter, R. P. & Noyes, W. A., Jr. 1959 *J. Amer. Chem. Soc.* **81**, 2307.
Pritchard, H. O. 1953 *Chem. Rev.* **52**, 529.
Russell, K. E. & Simons, J. 1953 *Proc. Roy. Soc.* A, **217**, 271.
Schüler, H. & Krimmel, E. 1957 *Z. Naturforschg.* **12** A, 528.
Wetmore, O. C. & Taylor, H. A. 1944 *J. Chem. Phys.* **12**, 61.
Wiig, E. O. & Kistiakowsky, G. B. 1932 *J. Amer. Chem. Soc.* **54**, 1806.
Wilkinson, P. G. & Johnson, H. L. 1950 *J. Chem. Phys.* **18**, 190.
Zelikoff, M. & Aschenbrand, L. M. 1956 *J. Chem. Phys.* **24**, 1034.
Ziskin, M. C. & Kondratiev, V. N. 1936 *Zh. Expt. Fiz.* **6**, 1083.

PROCEEDINGS OF THE ROYAL SOCIETY A MATHEMATICAL, PHYSICAL & ENGINEERING SCIENCES